Laboratory tests for the evaluation of the heat distribution efficiency of the *Friendly-Heating* heaters

Chiara Bertolin [a,*], Andrea Luciani [b], Luca Valisi [b], Dario Camuffo [a], Angelo Landi [b], Davide Del Curto [b]

[a] *Institute of Atmospheric Sciences and Climate (ISAC), National Research Council (CNR), Padova, Italy*
[b] *Politecnico di Milano, Department of Architecture and Urban Studies (DAStU), Milano, Italy*

Received 3 April 2015
Received in revised form 25 July 2015
Accepted 1 August 2015
Available online 4 August 2015

1. Introduction

The main purpose of the European Project Friendly-Heating (FH), active 2002–2005, was to study a specific heating method compatible with the conservation of cultural heritage objects, aiming at warming people while leaving church and artworks almost undisturbed in their natural microclimate. This strategy was preferred after comparisons with the other heating systems, by optimizing the pros and reducing the cons. The FH Project selected as case studies two churches in the Dolomite mountains, Italy, with very cold indoor climate, i.e. Rocca Pietore and Santo Stefano di Cadore, to rigorously test the compatibility between preservation needs and thermal comfort for the novel heating system.

The heat sources used in the Friendly Heating project, the thermal comfort on people and the potential impact on pews and on artworks were already studied with laboratory tests, field surveys and model simulations, and the results published in a number of papers [1–5]. In particular, vertical profiles of temperature (T) were monitored using a precision radiometer on a blackbody strip target of the same dimension as a standing person and using a black globe thermometer. This measurement technique required a number of sampling points over a regular grid on the blackbody strip target placed in proximity of the benches. Although each sampling was rapid, e.g. a few seconds, the total monitoring interval lasted a few minutes and some minor fluctuations were possible in the case of turbulence generated by the operator or thermal unbalances in the room.

In order to assess the full 3D heat efficiency distribution of the FH heaters, during the European Project Climate for Culture (CfC), active 2009–2014, laboratory measurements were carried out over a blackbody area using a precision infrared camera. Thermal images of the heat source and of the blackbody area were taken in order to represent all the grid points in the same instant to reduce the sampling time, thus avoiding the disturbance of local air motions and related temperature fluctuations.

This paper presents the results of the laboratory tests performed during winter 2013 and compared with the real case studies.

2. Methodology

2.1. Re-analysis of the case study

The 15th century church of S. Maria Maddalena in Rocca Pietore, situated at 1143 m above mean sea level, is a small massive

* Corresponding author. Tel.: +39 3208133245.
E-mail address: c.bertolin@isac.cnr.it (C. Bertolin).

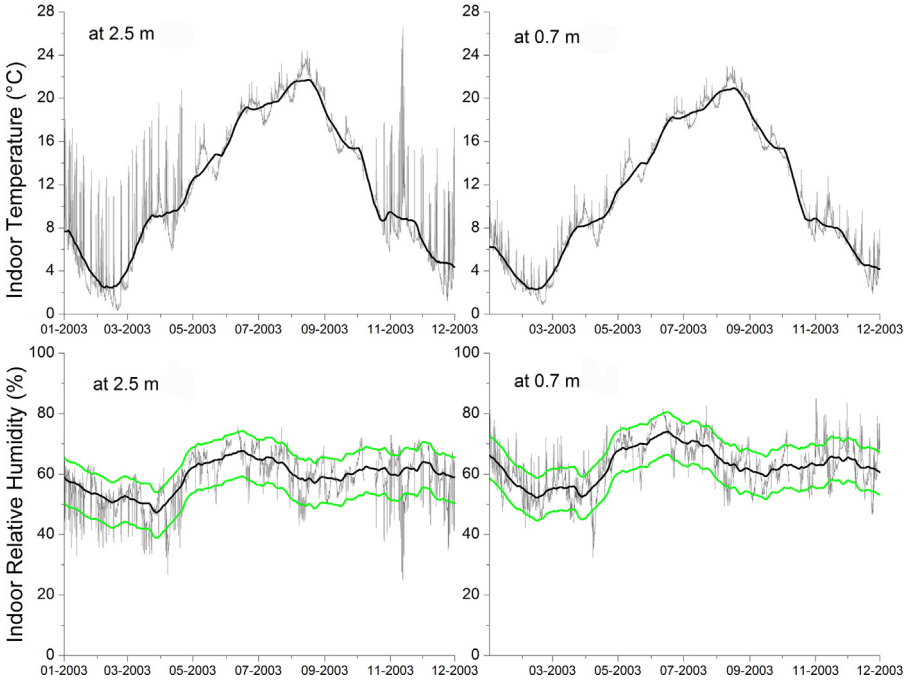

Fig. 1. Top panels: indoor temperature at 2.5 m (left) and 0.7 m (right) above the church floor monitored in the S. Maria Maddalena church at Rocca Pietore for the calendar year 2003. Thick black line 30 days running average (RA). Bottom panels: indoor Relative Humidity at 2.5 m (left) and 0.7 m (right). Thick black line 30 days RA. Thick light green lines 7th and 93rd percentile of the RH fluctuations. (For interpretation of the references to color in this figure legend, the reader is referred to the web version of this article.)

building, 25 m long, with one-meter-stone-thick walls. The nave is 8 m wide and 9 m tall, while the two side chapels are square, with each side measuring 4.5 m. The church contains several artworks: wooden altarpieces, paintings on canvas and panels, choir stalls, a decorated organ-loft with a modern organ, and frescoes. Before the FH Project, the church was provided with warm-air (WA) heating, planned for occasional use, mainly once or twice a week, for around 100 min of operation to mitigate the rigid outdoor winter temperature with minima ranging between −10 and −20 °C. Two grilles, one in the side chapel and the other in the nave (featuring blown-air velocities of 2.7 m/s and 0.4 m/s, respectively), supplied warm air (70–80 °C) inside. After a certain period the WA heating was in operation, some cracks on wood artworks increased in width, disfiguring the faces of the figures of St. Mary Magdalene and St. Catherine in the central part of the altarpiece. The FH monitoring campaign carried out from November 7th 2002 until June 3rd 2004 measured the environmental conditions that caused such dangerous events. Such campaign provided us with the 13-months monitoring data necessary to define the Historic Climate (HC) required for preventive conservation, as stated in the European Standard EN 15757:2010 [6]. Fig. 1 reports the indoor conditions re-analyzed in term of historic climate at two different heights, 0.7 m and 2.5 m respectively. The T and relative humidity (RH) values at these levels highlight the air stratification inside the church with stronger temperature peaks and relative humidity drops at higher level when the warm air heating system is in operation. The historic climate reconstruction shows that, during winter, the indoor average temperature is about 6.5 °C at 2.5 m and about 5.5 °C at 0.7 m, while the safe band (i.e. the 7th–93rd percentile of the fluctuations) of indoor relative humidity ranges between 40% and 68% at 2.5 m and 45–70% at 0.7 m. At the higher level (i.e. 2.5 m) RH drops cause shrinkage to wooden objects while at the lower level (i.e. 0.7 m) RH rises cause swelling.

The Church of Santo Stefano di Cadore is also a small massive stone church with three naves, small windows and thick walls. The church was funded in the 13th century, rebuilt in 1684 and a neo classic facade with columned arcade (i.e. pronaos) was added in 1817. It includes a precious organ, paintings and wooden statues. The church inside is some 20 m long, 10 m wide and 8 m tall. The site is at 950 m above the mean sea level, in the middle of a cold valley surrounded by snowed mountains.

Data were re-analyzed using the specific risk assessment tool developed by Martens in 2012 [7] within the CfC Project. The risk for mechanical damage on the wooden base material was assessed for three types of objects preserved inside churches: panel paintings, furniture and statues (Fig. 2).

For panel paintings, the Mecklenburg's plot [8] was used to assess mechanical damage caused by moisture gradients by determining whether yield occurs. The axes in the plot show the starting RH surface response (y axis) versus final RH full response (x axis). The panel is in safe conditions when its response to the environmental changes remains in the dark grey elastic region; deformation can eventually occur with plastic deformation on the panel (i.e. dots in the light grey area of the plot); finally cracks are likely to occur when the response falls in the failure region (i.e. grey area in the plot).

For furniture a similar approach was used, but over the Bratasz's plot [9] with full response RH (y-axis) and annual mean RH (x-axis). Elastic behavior is safe (i.e. dark grey area in the plot) while plastic behavior might cause damage (i.e. light grey area).

Finally, for wooden sculpture Jakiela's plot [10] for sloped RH changes was used to assess the risk induced by RH gradients. The level of risk for panel paintings, furniture and statues hypothetically placed at distance (d) from the tested heaters has been assessed and reported in Table 1.

The CfC mechanical risk analysis applied to the Rocca Pietore case study reported in Fig. 2 confirms that the central warm air-heating system was not sustainable for conservation as it gave rise to mechanical damages on wooden artworks contravening

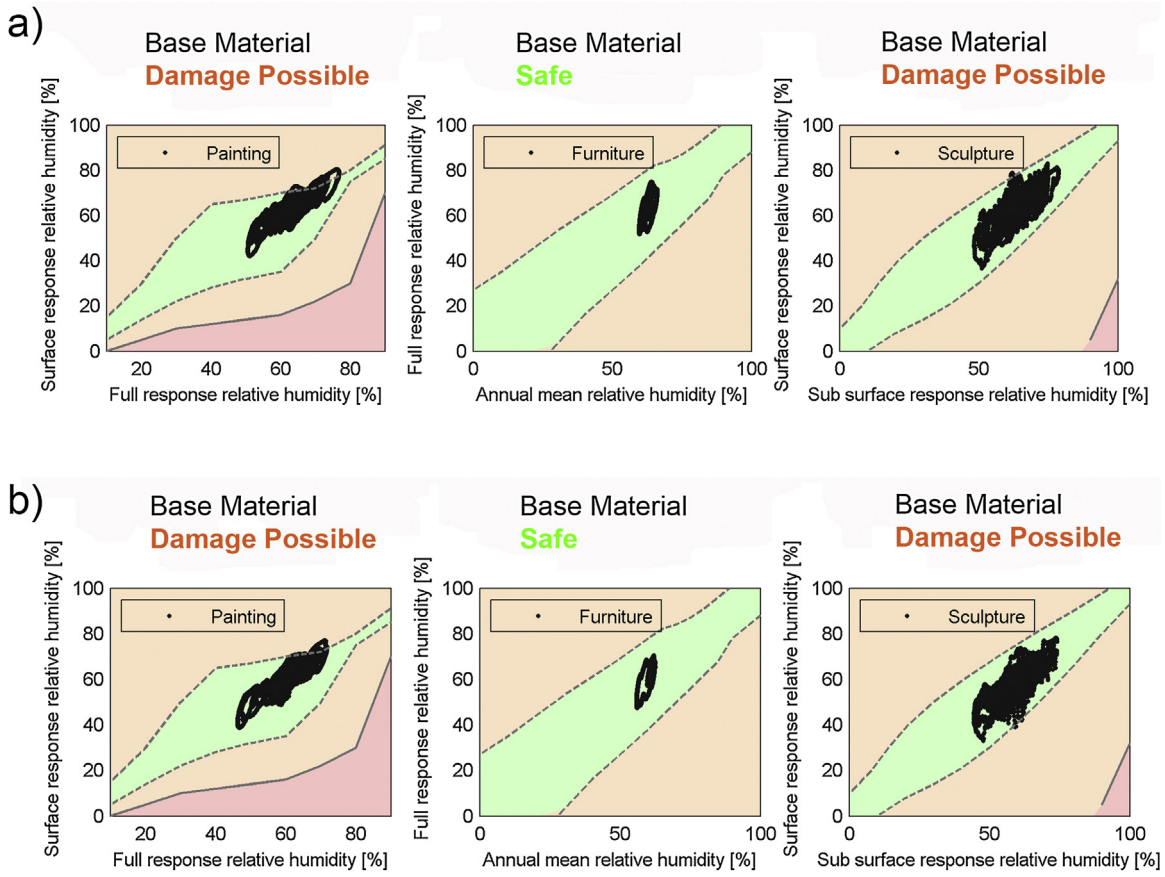

Fig. 2. Climate induced risk for 3 specific wooden objects preserved inside the S. Maria Maddalena church (i.e. panel painting (left), furniture (centre) and sculpture (right)) evaluated using the risk assessment method developed by Martens [7] within the CfC Project. (a) Indoor risk assessment at 0.7 m above floor, (b) indoor risk assessment at 2.5 m above floor.

the standard EN15759-1 [11] which states that in case of conflict between thermal comfort and conservation, the latter has priority. The approach used by the FH Project in planning a local heating strategy that leaves the church and the artworks undisturbed while at the same time provides an acceptable thermal comfort for people has shown to be a beneficial system both in terms of preventive conservation and energy saving. Moreover, Fig. 3, highlights as the daily thermos-hygrometric variations induced by the operation of the FH system with respect to the historic climate [6] falling within the safe band of RH fluctuations and maximum T variability. On the other hand, the central warm air heating events fall far beyond the historic climate.

Table 1
Level of risk for panel paintings, furniture and statues hypothetically placed at distance (d) from the tested heaters assessed using the damage functions available in literature.

Mechanical damage: Risk assessment method		Panel painting			Furniture			Statue		
		Determine whether yield occurs by using the Mecklenburg's plot [8]			No risk for RH changes <15% independent from change duration. If exceeded further analysis using the Bratasz's plot [9]			Determine whether reversible or irreversible response occurs by using the Jakiela's plot [10]		
Risk induced by position (d in cm) of heaters		Exp1	Exp2	Exp3	Exp1	Exp2	Exp3	Exp1	Exp2	Exp3
Element a	Safe	$d \geq 15$ cm	–	–	$d \geq 12$ cm	–	–	$d \geq 12$ cm	–	–
	Medium	$d \approx 12$ cm	–	–	$d \approx 10$ cm	–	–	$d \approx 10$ cm	–	–
	Risk	$d \leq 10$ cm	–	–	$d \leq 8$ cm	–	–	$d \leq 6$ cm	–	–
Element b	Safe	$d \geq 25$ cm	$d \geq 25$ cm	$d \geq 40$ cm	$d \geq 20$ cm	$d \geq 30$ cm	$d \geq 46$ cm	$d \geq 30$ cm	$d \geq 32$ cm	$d \geq 48$ cm
	Medium	$d \approx 15$ cm	$d \approx 15$ cm	$d \approx 35$ cm	$d \approx 12$ cm	$d \approx 20$ cm	$d \approx 38$ cm	$d \approx 20$ cm	$d \approx 20$ cm	$d \approx 30$ cm
	Risk	$d \leq 12$ cm	$d \leq 12$ cm	$d \leq 30$ cm	$d \leq 7$ cm	$d \leq 8$ cm	$d \leq 25$ cm	$d \leq 6$ cm	$d \leq 6$ cm	$d \leq 10$ cm
Element c	Safe	$d \geq 25$ cm	$d \geq 15$ cm	$d \geq 15$ cm	$d \geq 25$ cm	$d \geq 15$ cm	$d \geq 15$ cm	$d \geq 30$ cm	$d \geq 20$ cm	$d \geq 15$ cm
	Medium	$d \approx 15$ cm	$d \approx 7.5$ cm	$d \approx 6$ cm	$d \approx 15$ cm	$d \approx 7$ cm	$d \approx 7$ cm	$d \approx 15$ cm	$d \approx 12$ cm	$d \approx 10$ cm
	Risk	$d \leq 12$ cm	$d \leq 5$ cm	$d \leq 4$ cm	$d \approx 7.5$ cm	$d \leq 5$ cm	$d \leq 5$ cm	$d \leq 5$ cm	$d \leq 5$ cm	$d \leq 5$ cm
Element d	Safe	$d \geq 40$ cm	–	$d \geq 35$ cm	$d \geq 50$ cm	–	$d \geq 40$ cm	$d \geq 50$ cm	–	$d \geq 46$ cm
	Medium	$d \approx 35$ cm	–	$d \approx 25$ cm	$d \approx 30$ cm	–	$d \approx 25$ cm	$d \approx 30$ cm	–	$d \approx 28$ cm
	Risk	$d \leq 30$ cm	–	$d \leq 20$ cm	$d \leq 25$ cm	–	$d \leq 16$ cm	$d \leq 10$ cm	–	$d \leq 10$ cm

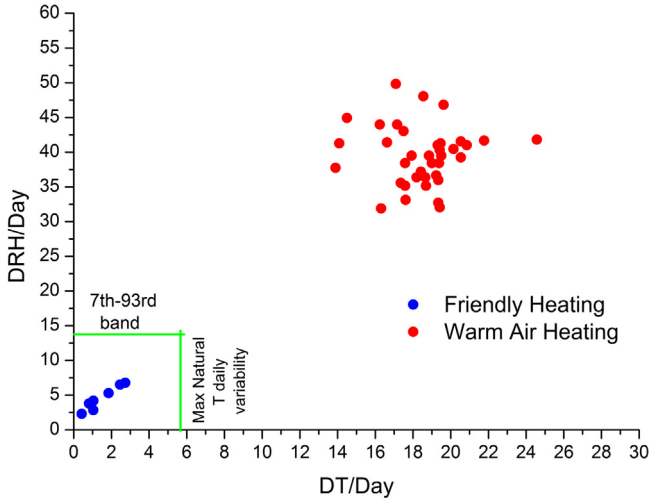

Fig. 3. Daily *T* and RH variation as measured during the operation of a warm air heating (red dots) and the friendly heating (blue dots) system. Green lines: limits of daily safe area constituted by the 7th–93rd percentile band of RH fluctuations [6] and the maximum natural *T* variability. (For interpretation of the references to color in this figure legend, the reader is referred to the web version of this article.)

2.2. Heaters tested

The FH strategy involves a number of low-temperature radiant sources ergonomically placed in the pews to heat various parts of the body (i.e. feet, calf and hands). The main idea is to reduce heat dispersion keeping the heat source localized and close to churchgoers, i.e. providing as much radiant area as possible for human comfort using modular heating elements fixed to the structural components of the pews.

This paper will analyze two basic heaters used in the Friendly-Heating project (in the following indicated FH) and two other commercial pew heaters with some similar characteristics (Fig. 4) as follows:

(a) Narrow heating foil strip (FH) enclosed in a rectangular iron sheet box fixed below the kneeler pad to heat feet from the upper side. It was used both in Rocca Pietore and in S. Stefano di Cadore. Electrical power: 50 W.
(b) Underseat FH heater with triangular section, heated with an electrical resistance and finished with a iron sheet. It was used in S. Stefano di Cadore. Electrical power: 210 W.
(c) Large heating foil (FH) bent into a half-cylindrical shape (i.e. semicircular section) and protected with a fine stainless steel mesh, fixed below the seat to heat calf. It was used in Rocca Pietore. Electrical power: 218 W.
(d) Commercial underseat heater with rectangular section, heated with an electrical resistance and finished with iron sheet, but with two open sides: i.e. the bottom and the front narrow side. The openings are protected with a grille to allow air circulation and warm calf. It is used in some churches but, after having made a comparison with the above mentioned prototypes, it was not considered neither for Rocca Pietore nor for S. Stefano di Cadore. Electrical power: 320 W.

The FH heating foil is made of an electrically heated layer of graphite in micro-granules deposited on a fiberglass support and then sealed between two plastic foils. When an electric current passes through the conductive graphite layer, the electrical energy is converted into heat energy and the layer gets heated up. Once the foil is heated, it swells and the increased width tends to increase the distance between granules. As a result, the electrical

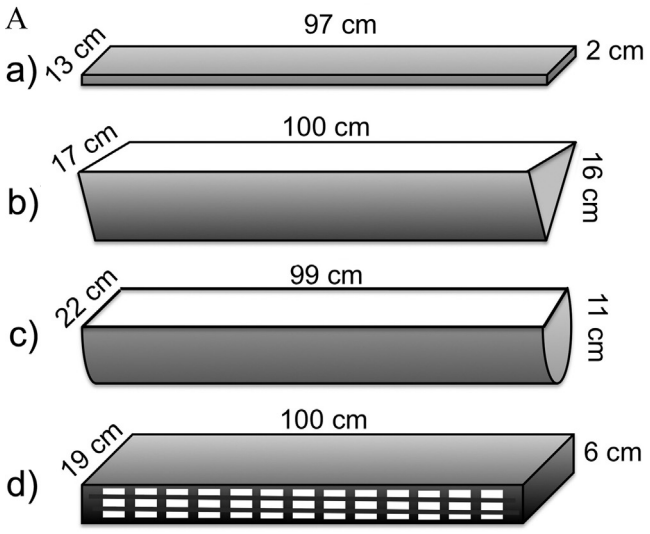

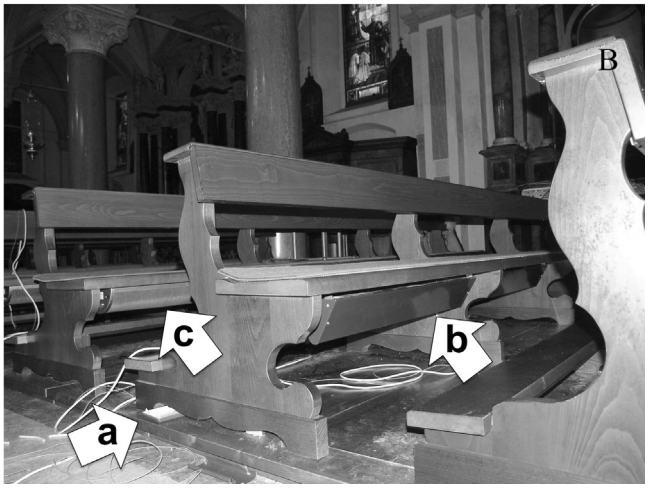

Fig. 4. a Heaters tested in this paper: (a) underkneeling FH heater composed of a narrow heating foil enclosed in a thin rectangular iron sheet box; (b) underseat FH heater with triangular section finished with a iron sheet; (c) underseat FH heater with semicircular section protected with a fine stainless steel mesh; (d) commercial heater with rectangular section finished with iron sheet, but with bottom and front opened for natural ventilation. The open parts are protected with a grille. b The triangular heater (b) and the semicircular (c) fixed below two seats of two pews during a winter test on the field. An underkneeling pad heater (a) not yet installed is partially visible lying on the floor, under the pew. The picture has been taken during the installation of the heaters to test their performances.

resistance increases with the foil temperature and reduces the current intensity. Consequently, the maximum temperature of the foil is self-regulated at specifically selected levels, established when the foil is built. This self-regulation provides a natural system cut-out that together with a thermostat for further fine regulation and safety, eliminates any risk of ignition or burning skin [2–5]. The FH heaters use heating foils. At close distance on the back of the heating foil, an aluminum foil (emissivity: 0.03 [12]), paral-lel to it, reflects the IR to increase the efficiency of the front side. Behind it an insulating panel avoids any overheating to the seat where the heater is fixed. The heating foil has an high emissivity of about 0.98 thus favoring the radiative emission and reducing the conductive–convective heat transfer that enhances convective air movements [2,5]. The front protection of the heating foil may be constituted of an iron sheet or a stainless steel grid.

In the case of an iron sheet frame, e.g. (a) and (b), the electrical resistance overheats the iron sheet envelope that emits IR radiation.

The emissivity is determined by the varnish type (typically in the range 0.87 to 0.94 [12]). The higher the emissivity, the weaker the convective air movements. When the front protection is a grid, the IR radiation passes through the grid empty spaces. The FH type (c) used a grid with 80% empty-to-full ratio. The IR impacting on the mesh is reflected and diffused. The stainless steel absorbance is very low (i.e. 0.07 [12]) so that only a negligible part of the radiation is absorbed by the mesh that never reaches burning temperatures but remains in the range 20–40 °C. At the end, some 83.5% of the feeding power is emitted as IR and 16.5% as air heating and convection.

Pew heaters are also composed of electrical resistances in the interior that transform the electric energy into heat. In the triangular heater (b) the core may be a common electrical resistance or a heating foil. The two V shaped lateral iron sheets are overheated and emit IR radiation, whilst the top side is thermally insulated and fixed to the seat.

In the commercial heater with rectangular section (d) the core is overheated at higher temperatures in comparison with the above heaters. The bottom and front are open but protected with grilles that allow the natural circulation of air moved by the thermal unbalance. In this way the main heat transfer mechanism is convection, and radiant heating is penalized.

In practice, the first three heaters tend to maximize radiant heating, while the type (d) is focused to produce a remarkable convection. However, from the point of view of comfort the presence of warm/cold draughts in a cold environment is a negative factor [1,2,4,5,13]. In addition, during the Friendly-Heating project it has been noted that the most effective local heating is obtained with IR thermal radiation as the warm air quickly escapes from the manned area and is dispersed aloft. Warm air is convenient for central heating, not for local heating.

The emission of the first three heaters is represented in Fig. 5, where the circle with arrow indicates the Lambert Law of IR emission: the radiant flow is maximum in the direction perpendicular to the emitting surface and decreases with the cosine of the angle formed with the normal to the surface.

The FH heater (a) with thin rectangular section is planned to be fixed behind the kneeling pad to heat feet placed under it, i.e. the front BB in Fig. 5. The radiant flow is maximum in the direction perpendicular to the emitting surface but is minimum and vanishes at grazing angle, giving a small dispersion on the side.

The heater with triangular section (b) offers the same radiant surface either frontally or laterally, providing the same IR contribution. It is aimed to heat the calf of people sitting in the equipped pew, and the front of legs of people sitting in the pew behind. How-ever, the heater surface is seen with an impact angle of 30° from the
normal, either in frontal or lateral position, so that the intensity is penalized by $\cos 30^\circ = \sqrt{3}/2$. The triangular form has been devised to allow a close position of calf.

The FH heater with semicircular section (c) is conceptually similar to the triangular (b) but it has been studied to optimize all advantages, as follows: (i) The internal heating foil is hot, but the protection grid absorbs just a little heat; the grid remains mild, avoiding any danger of burning. (ii) The emissivity is slightly higher for the above choice of the materials used for the emitting surface and the protection grid, thus increasing the efficiency. (iii) The cir-cular shape of emitting surface favors lateral emission at the top, i.e. most important level, where the emitting surface becomes ver-tical. (iv) The heating foil is very thin, i.e. 0.8 mm and has a very low thermal inertia. When it is warmed, it generates some con-vective air motion that is slowed down by the dynamic friction with the grid and the draught velocity is less than the triangle (b) that instead has smooth sides. The cold air enters from below and slightly cools the lower part of the heating foil, thus reducing the thermal emission toward the floor. The thin air layer slowly flows upwards along the foil gaining heat and thus reducing the heat

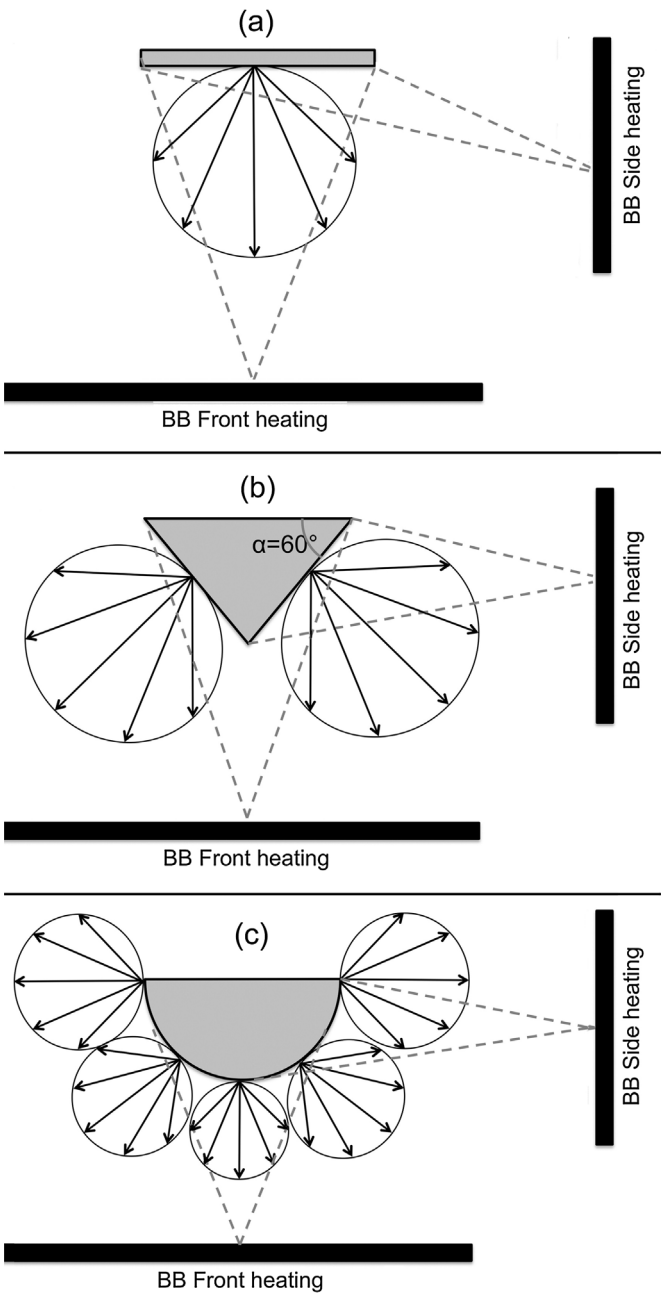

Fig. 5. IR emission of: the FH heater (a) with rectangular section; the FH heater (b) with triangular section; the FH heater (c) with semicircular section. BB is the blackbody strip positioned in the front and side of the heaters. The circle indicates the IR emission according the Lambert's cosine law.

subtracted by conduction from the foil. In the upper part of the curved foil the temperature is higher and this causes a further increase of the thermal emission toward legs. This dynamic air flow around the heater is reported in Fig. 6 together with the comparison with the element b.

2.3. Experimental methodology to assess the spatial variation of FH heaters thermal efficiency

Three experiments (Fig. 7) have been planned and implemented during winter 2013 in an indoor environment under natural unheated conditions i.e. 10 °C mean room temperature and rel-ative humidity ranging from 52% to 80%. These indoor *T* and RH conditions are representative of average winter levels in churches

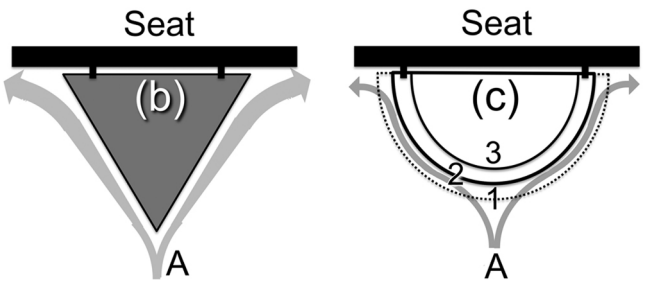

Fig. 6. Dynamic airflow A that forms around heaters when operating. The heaters (b) and (c) are represented fixed below pew seats. The triangular heater (b) has smooth V sloped sides and forms intense draughts. The semicircular heater (c) is composed of an external fine-mesh grid (1, dotted line), the heating foil (2, thick line) and the inner reflecting aluminium foil (3, thin line). The air penetrates from below and may flow in the free space between the grid and the heating foil, but the air motion is slowed by the large friction with the grid. This ventilation lowers the temperature of the foil when cold air enters from the bottom; it warms over the path and increases the temperature on the upper part of the foil and in the back is thermally insulated to avoid dispersion by a reflecting aluminium foil.

located in mild climate where pew heating can provide good thermal comfort. In the case of very cold climates, the local heating may be helpful, but must be integrated with heavy clothing.

The experimental methodology was based on remote sensing measures of the surface temperature of a Black Body (BB) target area using an infrared (IR) thermocamera.

The BB target method [4,5,14,15] is an efficient experimental approach to measure vertical and/or horizontal gradients of effective temperature due to the synergism of air temperature, visible and infrared radiation and convective air motions in the position where the target is located. Such target simulates the temperature experienced by a churchgoer of which we want to assess the received level of thermal comfort as well as a valuable object we need to preserve (e.g. paintings on canvas, wooden panels or tapestry) in the church.

Therefore, most of the materials used for cultural property can be represented by a BB target area with a fixed high emissivity value, except for polished metals that have a very low emissivity and reflect most of the incoming radiation.

The BB target used in the experiments was built in accordance with EN 15758:2010 [14] and had the following features:

- it was a surface of black textile with a rectangular shape (100 cm length, 80 cm width);
- it was opaque to visible and IR radiation, i.e. it showed neither light nor IR transmission;
- it had high emissivity i.e. 0.94; and
- it had low thermal inertia to ensure a short response time.

During the experiments four heaters were tested one at a time under regime conditions. For each heater a set of IR images, together with the room conditions at that instant, were recorded at distances gradually closer to the BB target area.

The effective temperatures resulting from the thermal balance between air temperature and radiation were determined with fast and accurate measurements of the BB target using a FLIR P620 model infrared camera. There are two types of errors of a temperature measurement performed with a thermal cameras: The external errors and the intrinsic errors. Usually the producer gives notices of camera performance when only the intrinsic errors are present (i.e. accuracy as a range in which the output temperature is located around the true object temperature). Such a situation is achievable when emissivity of the tested object is close to unity and a camera-object distance is short, which they are the conditions under which the tests were done. The external errors due to unknown emissiv-ity, reflected radiation and limited atmospheric transmittance can be treated as negligible. The accuracy of the instrument is ± 2 °C in operating conditions ranging from -15 °C to +500 °C, while the detector is a FPA uncooled micro bolometer with a resolution of 640 $\times$ 480 pixel. Room conditions (i.e. air temperature and relative humidity) at the instant of measurement were measured with an EXTECH M0297 digital hygrometer. It has a rather limited accuracy (T: ± 2 °C; RH: $\pm 2.5\%$), but it can be connected via bluetooth with the infrared camera, allowing a realtime correlation between thermal image and room air T and RH. In order to assess the hygrothermal behavior at the interface between air and BB target area, a computer processing was carried out on all the IR images recorded during the experiments, consisting each one of a matrix of effective temperature data. Each of these matrices was reproduced in terms of 2-D RH surface representation. This has been calculated, pixel by pixel, after the computation of the humidity mixing ratio (MR) close to the surface and the surface temperature captured from the IR thermal image [5,16].

The final outcomes of such computer processing was elaborated as false colour images.

The uncertainty for the mixing ratio has been calculated using the general error propagation formula:

$$\partial \mathrm{MR}(T, \mathrm{RH}) \leq \left|\frac{\partial \mathrm{MR}}{\partial T}\right| \partial T + \left|\frac{\partial \mathrm{MR}}{\partial \mathrm{RH}}\right| \partial \mathrm{RH} \quad (1)$$

from the classical error theory [17] applied at the MR equation as function of measured T_{room} and $\mathrm{RH}_{\mathrm{room}}$ values.

$$\mathrm{MR} = 38.015 \times \frac{10^{(7.65\times T)/(243.12+T)} \times \mathrm{RH}}{1000 - \left(0.06112 \times 10^{(7.65\times T)/(243.12+T)} \times \mathrm{RH}\right)} \quad (2)$$

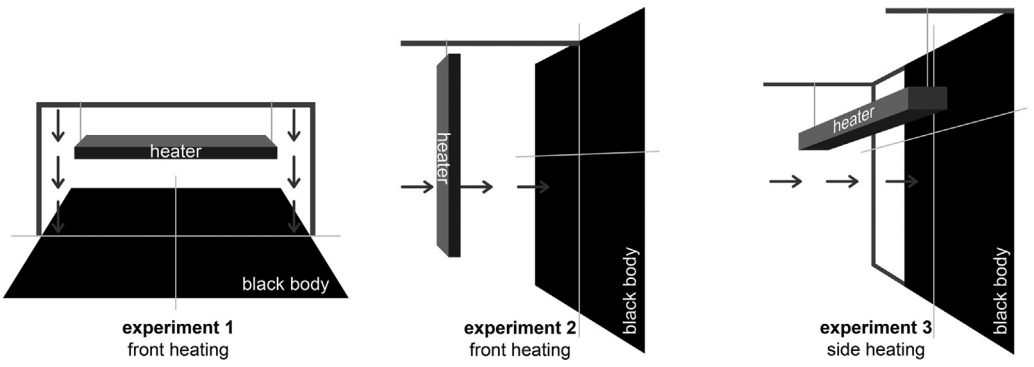

Fig. 7. Scheme of the three experiments performed in winter 2013 during the Climate for Culture Project to test the directionality of the radiant efficiency of the heaters. The term black body refers to Black Body Target area as described in the standard EN15758:2010 [14].

Finally the relative humidity uncertainty has been calculated with (1) using the following equation:

$$RH = \frac{1000 \times MR}{10^{((7.65 \times T_{BB})/(243.12+T_{BB}))} \times (38.015 + 0.06112 \times MR)} \quad (3)$$

as function of mixing ratio and black body surface temperature as measured by the thermocamera.

The results are reported in Table 2 and estimate the limit errors i.e. a range around the result of measurement in which the true value of the measured quantity is located with high value of probability.

Scope of the experiments was to test the influence of the geometric shape of the heaters on directionality of the radiant efficiency, i.e. the difference in efficiency between the front and side use of the heaters.

The experimental results were comparable for the triangular (b) and semicircular (c) heaters only, because they have similar characteristics in shape and electrical power. The final comparison between the experiments has not been applied to the other heaters because they are less homogeneous.

3. Results and discussion

3.1. First experiment

In the first experiment, all the heaters in Fig. 4a were tested for the front heating evaluation (Fig. 7—left scheme). Front heating is especially relevant for FH (a) aimed to feet heating (i.e. positive fac-tor) or for some particular use of other heaters. However, when the heaters (b) (c) and (d) are fixed in their normal position under the seat, the frontal heat reaches the floor and constitutes dispersion (i.e. negative factor). During the experiment, the heaters are kept horizontally, with the front heating surface parallel to the BB that is located on a horizontal plane. In this condition, the BB warm-ing is only due to thermal IR emission, because the air warmed by contact with the heater surface goes aloft. After each acquisi-tion of the IR thermal image, the distance between the heater and the target surface is gradually reduced moving the element ver-tically. The heating efficiency decreases with increasing distance, as shown by the difference in temperature between the BB tar-get area and the room. IR measurements and computer simulation processed to gain images of the RH at the air-BB target area inter-face are reported in Fig. 1 of the online Supplementary material to show the potential effect in lowering the relative humidity at the interface between a wooden panel, or a painting on canvas, and the air.

The two-dimensional T and RH images report the spatial distribution of heat on the BB target area. Semicircular (c), triangular (b) and the kneeler pad (a) heaters provide a similar effect on the target surface, when the distance from the heater exceeds 25 cm. At shorter distances, the behavior follows the peculiar heating efficiency of the element with a better performance of the most powerful (i.e. 320 W) rectangular underseat heater (d) (Fig. 1d Sup-plementary material) compared to the others (i.e. about 210 W in Fig. 1b and c of Supplementary material). The higher efficiency is also justified because this element has a hot core and the bottom is open, except for the protection grille. Moreover the semicircular and the triangular heaters heat a larger area respect to the above heaters and the kneeler pad heater. It should be mentioned, how-ever, that the surface area of the kneeler pad heater is much smaller than the horizontal section of the others i.e. from 60 to 80% less, and its power is less than 25% of the others.

The front heating efficiency observed in the laboratory is reported in Fig. 8. The result represents the radiant heat reaching

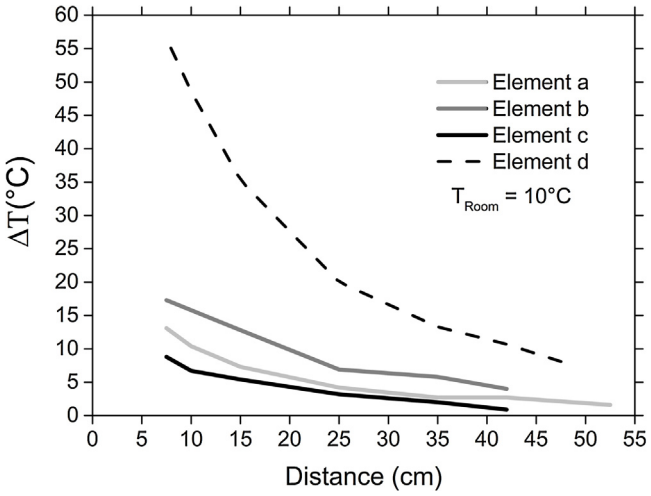

Fig. 8. Results of the 1st CfC experiment. The plot shows the front heating efficiency (BB vertical approach) for the underkneeling (a), triangular (b), semicircular (c) and commercial heater (d) at room temperature ranging of 10 °C as in the legend.

the floor, i.e. lost to the aim of comfort. The triangular heater (b) has higher floor dispersion than the semicircular heater (c).

3.2. Second experiment

In the second experiment the front heating efficiency has been assessed for heaters kept in vertical position and aiming to heat a person in front of them. The comparison is made between the two heaters with the same power consumption and similar size (i.e. the semicircular (c) and triangular (b) elements). The heaters are hung vertically, with the front heating surface parallel to the BB target area that is now located on a vertical plane. In this condition, the air warmed by contact with the heater surface rises forming a thin dynamic boundary layer that flows vertically along the heater. The distance of the BB from the heater is gradually reduced, moving horizontally the heating element (Fig. 7—central scheme). The read-ings are representative of the thermal IR emission of the heater, the convective effect being limited to a thickness of a few centimeters from the hot surface. The two sets of IR measurements and RH cal-culated images are reported in Fig. 2 of the online Supplementary material. During the operation, the semicircular element, warms a larger area on the upper edge of the target surface, this effect being emphasized by the higher temperatures reached on the upper part of the heater for the convective flow along the surface. On the other hand the triangular element has a symmetric space distribution of the radiation respect to the vertical axis of the target surface.

Fig. 9, reports the front heating efficiency of the two heaters. Under this experimental setup, the semicircular underseat heating is proved to be 70–100% more efficient than the previously tested position (Section 3.1), the distance of maximum efficiency being within 30–35 cm from the target surface. On the contrary, the triangular underseat heating element loses 50% efficiency respect the position tested in Section 3.1. This experiment makes a comparison of the two heaters in terms of the heat usable for thermal comfort. The FH semicircular heater is between 50% and 75% more efficient than the triangular one with a maximum efficiency within 15 cm from the target surface. The difference is justified by the effect of the dynamical airflow that develops along the warm surfaces, as discussed in Section 2.2.

3.3. Third experiment

In the third and last experiment the side heating efficiency is measured for the 2 FH heaters with the same power consumption

Table 2
Uncertainties related to the instruments used to perform measurements and estimated by calculation applying the general error propagation formula [17].

Variable	Instrument	Uncertainty
T_{BB} (measured)	FLIR P620 infrared camera*	±2% or ±2 °C in operating conditions ranging from −15 °C to +500 °C
T & RH room conditions (measured)	EXTECH M0297 digital hygrometer	±2 °C, temperature ±2.5%, relative humidity
Room mixing ratio (calculated)	Input: T_{room} & RH_{room}	±0.5 g/kg
RH_{BB} (calculated)	Input: MR_{room} & T_{BB}	≤10% in the T_{BB} experimental range (4)Uncertainty(%) = $19.5 \times \exp\left(\frac{-T_{BB}}{14.6}\right) + 0.25$

* Calibration certificate from the producer.

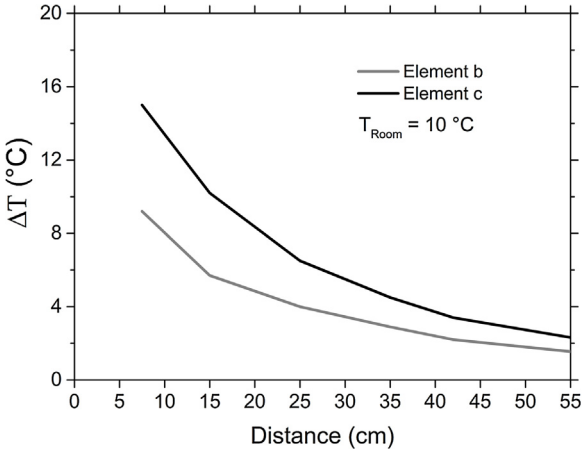

Fig. 9. Results of the 2nd CfC experiment. The plot shows the front heating efficiency (BB horizontal approach) for the triangular (b) and the semicircular FH heater (c) at room temperature of 10 °C as in the legend.

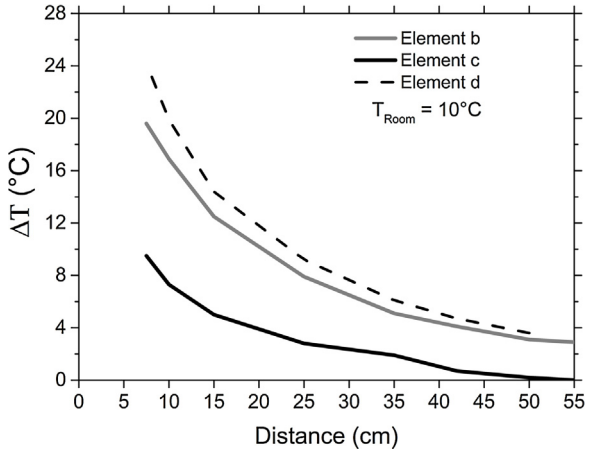

Fig. 10. Results of the3rd CfC experiment. The plot shows the side heating efficiency (BB horizontal approach) for the 3 heaters (i.e. triangular (b), semicircular (c) and commercial heater (d)) at room temperature ranging from of 10 °C as in the legend.

(i.e. semicircular and triangular shape with 220 W power supply) and for the rectangular underseat heating element with 50% more power supply, i.e. 320 W. During the test, the heaters are kept horizontally, with the heating side parallel to the BB target area that is located on a vertical plane. In this condition, the air warmed by con-tact with the surface of the semicircular and the triangular heaters rises forming a dynamic boundary layer that flows along the heater with a horizontal component of the momentum. The dynamic sit-uation and the turbulence tend to spread heat at a certain distance from the heaters. The rectangular element with free ventilation on the bottom and the front acts as a chimney. In this experiment, the distance of the heater from the BB target is gradually reduced, moving the heater on the horizontal plane.

It should be underlined that for this experiment the BB target area was not enough extended to cover all the heated area. As heaters heat symmetrically on either sides, it was decided to expose the target area in front of half the heater surface (Fig. 7—right scheme). The three sets of measurements are reported in Fig. 3 of the online Supplementary material. The element that provides the most extended heated area is the rectangular one for the larger distance reached by the momentum gained for the chimney effect.

Under this configuration, the radiant efficiency simulated at room temperature of 10 °C is reported in Fig. 10. The side heating is higher for the powerful rectangular underseat heater although, despite its power supply, it is only 20% more effective than the trian-gular underseat heating element. The semicircular element shows the same behavior as in experiment 1 in Section 3.1.

The results of this configuration are difficult to interpret because the heaters kept in horizontal position, for their particular section, form on both sides a flow of air with a horizontal momentum that tends to expand laterally, at least at the short distances of the test. In this case the radiant and the advection contributions cannot be easily separated and only the overall effect is visible. The higher temperature increase is due to the triangular heater, but we know that it also generates the more intense airflow.

3.4. Comparison between the experiments

A comparison of results obtained in Section 3.1 (experiment 1) and Section 3.3 (experiment 3) under condition of T_{room} = 10 °C is reported in Fig. 11. Fig. 11—top panel, highlights the preferable installation position of the triangular underseat heating element. This element has its maximum performance when installed horizontally with the side heating-surface radiating the target area placed on a vertical plane (experiment 3 in Section 3.3). Under this experimental setup, at 10 °C room temperature a ΔT = 8 °C is still reached at a distance of about 25 cm. Fig. 11—center panel, reports the performances of the semicircular underseat heating element. It has been conceived for underseat use, i.e. kept horizontally, but also to be installed vertically in some special cases, e.g. the choir. The heating efficiency increases when it is installed vertically with the front heating surface radiating the target placed on a vertical plane (experiment 2 in Section 3.2). In such condition and with T_{room} = 10 °C, a ΔT = 8 °C is reached at a distance of about 25 cm. Fig. 11—bottom panel. The plot highlights that a good practice to reach an acceptable comfort level (e.g. ΔT = 8–10 °C temperature increase) is on a restricted area around pews, i.e. 5–10 cm maximum.

3.5. Temperature profiles and air draughts in churches

It is interesting to see the performances of the semicircular and triangular heaters in real conditions once installed in two churches with similar climate in the Italian Alps, respectively, S.

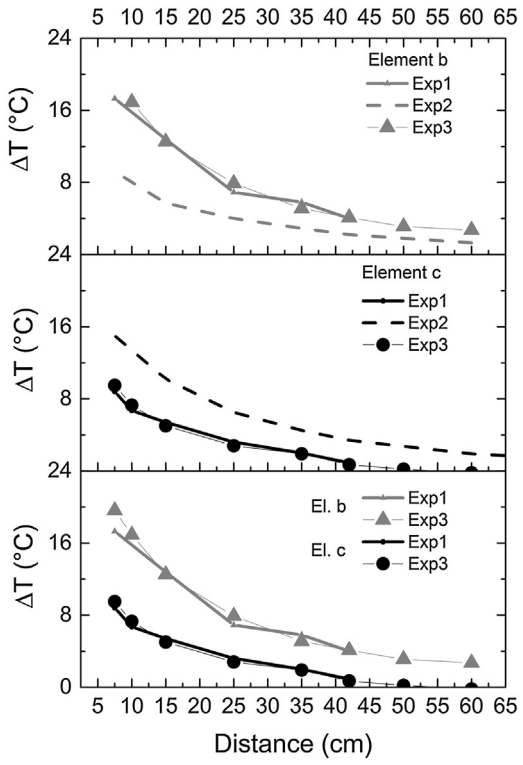

Fig. 11. Comparison between the CfC experimental results. Top Panel: Directionality of the radiant efficiency for the triangular (b) heating element. Central Panel: Directionality of the radiant efficiency for the FH semicircular (c) heating element. Bottom Panel: experiments 1 and 3 comparing the front and side heating for the triangular (b) and semicircular (c) heaters.

Maria Maddalena in Rocca Pietore and S. Stefano di Cadore. After the installation, the heaters were tested both in terms of warming efficiency at a fixed position (i.e. 30 cm that represents the space platform between one pew and the next) and in draughts generation using a Campbell Scientific ultrasonic anemometer to monitor the air movements at 95 cm above the heaters, which corresponds to the level of the face of a person sitting on pews. The ultrasonic anemometer measures the wind speed and direction on the horizontal and vertical directions, as well as the turbulent fluctuations of the wind field. The BB profiles in the pews are reported in Fig. 12a and the draughts in Fig. 12b.

In cold rooms the air movements are crucial in causing discomfort, vanishing the positive effect of heating. After the sonic anemometer records, a comfort parameter called draught rate (DR) has been calculated that represents a percentage of people feeling discomfort by draught. The DR parameter was introduced by Fanger [13] and then recommended by EN ISO 7730:2003 [18] and ANSI/ASHRAE 55:2004 [19].

Draught sensation depends on the air speed, air temperature, turbulence intensity, human activity and clothing. In a cool church, a draught may cause unpleasant sensation especially for the head and legs where the body is not covered with clothing. The DR [%] was calculated according to the two above standards using the following formula:

$$\mathrm{DR} = \left(34 - \bar{T_{\mathrm{Air}}}\right) \times \left(\bar{V_{\mathrm{Air}}} - 0.05\right)^{0.62} \times \left(0.37 \times V_{\mathrm{Air}} \times \bar{Tu} + 3.14\right) \quad (5)$$

where the variables are: T_{Air} is the average air temperature [°C], V_{Air} is the average air velocity [m/s], and $Tu = \sigma V_{\mathrm{Air}}/V_{\mathrm{Air}}$ is the average turbulence intensity [%].

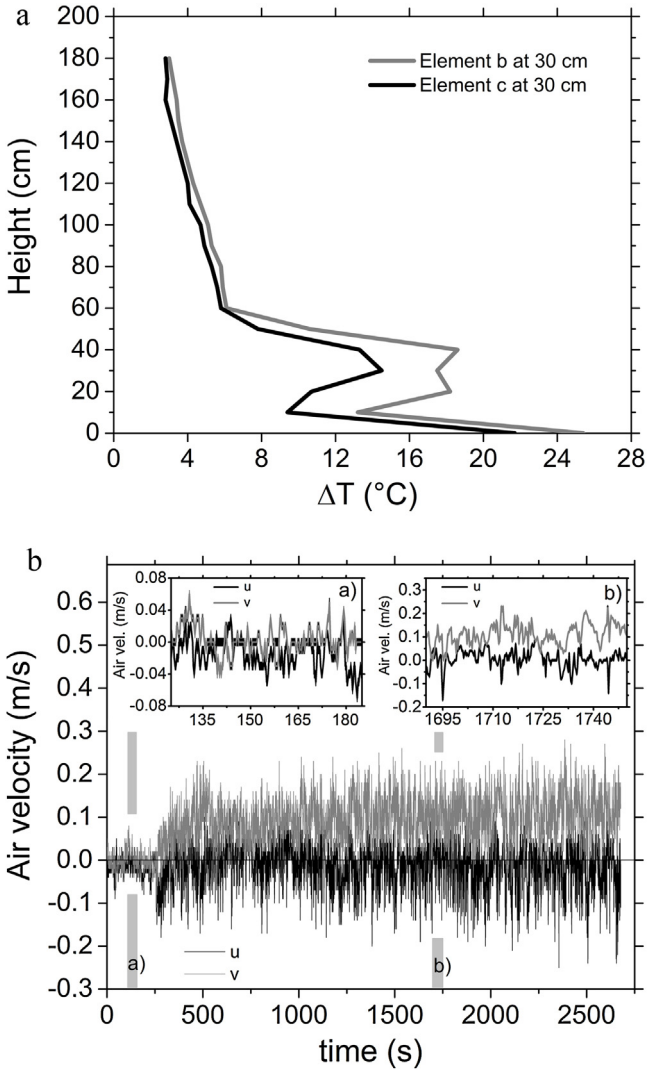

Fig. 12. (a) The triangular (b) and semicircular (c) heaters were tested in situ into the churches of S. Stefano di Cadore and S. Maria Maddalena in Rocca Pietore in terms of warming efficiency at a fixed position (i.e. BB profiles at 30 cm from the heater). (b) Main plot. Monitoring of the air movements at 95 cm above the heaters with an 2-D ultrasonic anemometer. Wind speed on the horizontal (v) and vertical (u) directions. Sub-plot (a) air movement monitored over one-minute time window when the heating systems were turned off. Sub-plot (b) air movement monitored over one-minute time window after the heating systems were turned on. The error band (i.e. ±0.5 cm/s) of the readings is inserted in the two subplots but still no readable.

DR is valid for sedentary, thermally neutral persons dressed in normal clothing in working rooms. Under these conditions, the recommended value is DR < 15% at $T = 18\,^{\circ}\mathrm{C}$. However, the real situation in a church is worst and higher DR levels should be expected. The measurements in the church of Rocca Pietore with semicircular heaters gave vertical air motions in the range $-15\ \mathrm{cm/s} < v < +15\ \mathrm{cm/s}$ and DR in the range $20\% < \mathrm{DR} < 30\%$, where DR = 20% was found in the pew area and the highest DR levels were found in proximity of the cold side walls [4]. The church had a warm-air heating system that was substituted by the FH pew heating and it was at times operated in order to recognize the differences between the two systems. When the warm air heating was operated the air movements were faster and DR increased in the range $45\% < \mathrm{DR} < 80\%$. The measurements in the church of S. Stefano di Cadore with triangular heaters gave air motions in the range $-20\ \mathrm{cm/s} < v < +20\ \mathrm{cm/s}$ and DR in the range $26\% < \mathrm{DR} < 30\%$.

In practice, in the real case, at ambient temperatures around 0 °C, the semicircular and the triangular heaters gave similar results in providing thermal comfort and in the percentage of people feeling discomfort by draught.

4. Conclusions

This paper reports the results of the re-analysis carried out on monitoring data acquired during the Friendly Heating Project (active 2002–2005) on two churches in the Italian Alps. This re-analysis applies two important tools for cultural heritage preservation which have been obtained in the years after the completion of the FH project: the concept of historic Climate stressed in [4,5] and standardized in EN15757 [6] and the specific risk assessment method developed within the CfC European Project concluded in 2014 [7,20]. The first tool allows evaluating the safe thresholds for cultural heritage collections in a specific environment, e.g. a church under unheated conditions or with local heating. The second one, allows assessing the risk for specific categories of objects and evaluate the hazardous nature of various heating strategies. On the background of the re-analysis results, the FH strategy has been demonstrated to be the best strategy meeting the EN15757:2010 [6] and EN15759-1:2011 [11] requirements.

For this reason, under the CfC Project, laboratory tests have been implemented to assess the heating efficiency of some heaters with different power consumption, geometric shape and dimensions.

Results are useful to assist final users with the installation to obtain the best compromise between comfort and artwork conservation [11] avoiding that IR radiation will exceed risk-thresholds for plastic deformation of wood or failure. In particular, the laboratory tests have been compared with the verification on real conditions with the heaters installed in two churches with similar local climate on the Alps. The triangular and the semicircular heaters provide similar results both in terms of heating and draught generation, when used in underseat position to warm calf and legs. Draughts generated by heaters constitute a serious problem: they are unpleasant and tend to reduce the comfort of heaters and to increase the deposition rate of suspended particulate matter, soiling frescoes and paintings. Increasing feeding power, one increases the heater temperature and the thermal comfort, but it increases the draughts too, with the result of losing any advantage or lowering the comfort sensation. The most effective local heating is obtained with IR thermal radiation, while warm air is a source of heat dispersion, this should be kept in mind when a church heating is planned.

Finally, the sustainability of the electric power consumption is another relevant feature. The energy consumption using FH prototypes for an intermittent localized strategy during services is 2.42 MW per year instead of the 20.79 MW per year required by a centralized warm air heating system used under the same conditions, which means that an energy saving of more than 88% can be obtained.

Acknowledgements

The Laboratory experiments and the data elaboration were carried out under the EU funded Climate for Culture Project (Grant 226973). The participation of the researchers from Politecnico di Milano was made possible by funds provided by the Scuola di Specializzazione in Beni Architettonici e del Paesaggio (Graduate School in Architectural and Landscape Heritage) of Milan.

The prototypes were developed under the EU funded project Friendly Heating (EVK4-CT-2001-00067) active 2002–2005, as well as the surveys in the churches of Rocca Pietore and S. Stefano di Cadore.

Appendix A. Supplementary data

Supplementary data associated with this article can be found, in the online version.

References

[1] D. Limpens-Neilen, Bench Heating in Monumental Churches—Thermal Performance of a Prototype, Eindhoven Technical University, Eindhoven, 2006 (PhD Thesis).

[2] D. Camuffo, E. Pagan, H. Schellen, D. Limpens-Neilen, R. Kozlowski, L. Bratasz, S. Rissanen, R. Van Grieken, Z. Spolnik, L. Benes, J. Zajaczkowska-Kloda, P. Kloda, M. Kozarzewski, G. Santi, K. Chmielewski, T. Jutte, A. Haugen, T. Olstad, D. Mohanu, B. Skingley, C. Saiz-Jimenez, C.J. Bergsten, A. della Valle, C. Don Russo, G. Bon Valsassina, C. Accardo, E. Cacace, A. Giani, M.P. Giovagnoli, A.M. Nugari, R. Pandolci, C. Rinaldi, Acidini C. Danti, A. Aldrovandi, R. Boddi, V. Fassina, L. Dal Pra, F. Raffaelli, R. Bertoncello, P. Romagnoni, M. Camuffo, A. Troi, Church Heating and Preservation of the Cultural Heritage: A Practical Guide to the Pros and Cons of Various Heating Systems, Electa Mondadori, Milano, 2007 (240 pp.).

[3] Ł. Bratasz, R. Kozlowski, D. Camuffo, E. Pagan, Impact of indoor heating on painted wood: monitoring the mediaeval altar in the church of Santa Maria Maddalena in Rocca Pietore, Italy, Stud. Conserv. 52 (2007) 199–210.

[4] D. Camuffo, E. Pagan, S. Rissanen, L. Bratasz, R. Kozlowski, M. Camuffo, A. della Valle, An advanced church heating system favourable to artworks: a contribution to European standardization, J. Cult. Heritage 11 (2010) 205–219, l0.1016/j.culturher.2009.02.008.

[5] D. Camuffo, Microclimate for Cultural Heritage—Conservation, Restoration and Maintenance of Indoor and Outdoor Monuments, second ed., Elsevier, New York, NY, 2014.

[6] EN, Conservation of cultural property—specifications for temperature and relative humidity to limit climate-induced mechanical damage in organic hygroscopic materials, in: EN 15757, European Committee for Standardization, Brussels, 2010.

[7] M.H.J. Martens, Climate Risk Assessment in Museums, Eindhoven Technical University, Eindhoven, 2012 (PhD Thesis).

[8] M.F. Mecklenburg, C.S. Tumosa, E. Erhardt, Structural response of painted wood surfaces to changes in ambient relative humidity, in: V. Dorge, F. Carey Howlett (Eds.), Painted Wood: History and Conservation, Getty Conservation Institute, Los Angeles, CA, 1998, pp. 464–483.

[9] Ł. Bratasz, R. Kozloswki, A. Kozlowska, S. Rivers, Conservation of the Mazarin chest: structural response of Japanese lacquer to variation in relative humidity, ICOM Comm. Conserv. 11 (2008) 1086–1093.

[10] S. Jakiela, L. Bratasz, R. Kozlowski, Numerical modeling of moisture movement and related stress field in lime wood subjected to changing climate conditions, Wood Sci. Technol. 42 (2007) 21–37.

[11] EN, Conservation of cultural property—indoor climate—Part 1: Heating chapels churches and other places of worship, in: EN 15759-1, European Committee for Standardization, Brussels, 2011.

[12] W. Wolfe, G.J. Zissis, The Infrared Handbook, Infrared Information and Analysis Center, Ann Arbor, MI, 1989.

[13] P.O. Fanger, Thermal Comfort, Danish Technical Press, Copenhagen, 1970.

[14] EN, Conservation of cultural property. Procedures and instruments for measuring temperatures of the air and the surfaces of objects, in: EN 15758, European Committee for Standardization, Brussels, 2010.

[15] D. Camuffo, C. Bertolin, V. Fassina, Microclimate monitoring in a Church, in: D. Camuffo, V. Fassina, J. Havermans (Eds.), Basic environmental mechanisms affecting tangible cultural heritage—understanding deterioration mechanisms for conservation purposes COST Action D42 "Enviart", Nardini, Florence, 2010, p. 178 (Chapter 3).

[16] H.L.H. Schellen, Heating Monumental Churches: Indoor Climate and Preservation of Cultural Heritage, Technische Universiteit Eindhoven, 2002.

[17] J.R. Taylor, An introduction to error analysis: The study of uncertainties in physical measurements., University Science Books, Mill Valley, Calif, 1982.

[18] EN, Moderate thermal environment—determination of the PMV and PPD indices and specification of the conditions for thermal comfort, in: EN ISO 7730, International Organization for Standardization, 2003.

[19] ANSI/ASHRAE, Thermal environmental conditions for human occupancy, in: ANSI/ASHRAE Standard 55, ANSI/ASHRAE, 2004.

[20] C. Bertolin, D. Camuffo, Deliverable 5.2. Climate for Culture EU Project—Grant Agreement No. 226973, 2014.